Simultaneous determination of nucleation and crystal growth kinetics of struvite using a thermodynamic modeling approach

Mary Hanhoun, Ludovic Montastruc, Catherine Azzaro-Pantel, Béatrice Biscans, Michèle Freche, Luc Pibouleau

Simultaneous determination of nucleation and crystal growth kinetics of struvite using a thermodynamic modeling approach

Mary Hanhoun [a], Ludovic Montastruc [a], Catherine Azzaro-Pantel [a,*], Béatrice Biscans [a], Michèle Frèche [b], Luc Pibouleau [a]

[a] Université de Toulouse, Laboratoire de Génie Chimique, UMR 5503, CNRS/INPT/UPS, BP 84234, INP-ENSIACET, 4 allée Emile Monso, 31030 Toulouse cedex 4, France
[b] Université de Toulouse, CIRIMAT, UMR 5085, CNRS/INPT/UPS, BP 44362, Campus INP-ENSIACET, 4 allée Emile Monso, 31432 Toulouse cedex 4, France

HIGHLIGHTS

- This work concerns the controlled struvite formation by precipitation.
- We model nucleation and growth kinetics.
- A thermodynamic model is coupled with a population balance.
- The model predicts particle size distribution vs. experimental time.
- It allows the identification of nucleation and particle growth kinetics parameters.

Keywords:
Struvite
Precipitation
Modeling
p-Recovery
Nucleation–growth
Population balance
Stirred reactor

ABSTRACT

This work concerns the controlled struvite formation ($MgNH_4PO_4{\cdot}6H_2O$) by precipitation as an alternative removal of phosphorus and, consequently, of ammonium from wastewater discharges. A new method, based on an integrated methodology, is proposed here for predicting and controlling struvite nucleation and growth rate. Experiments were conducted in an isothermal stirred batch reactor at a temperature of 25 °C from a synthetic aqueous solution at different pH levels (8.5–9.6). The initial concentrations of Mg, PO_4 and NH_4 are fixed at 3 mmol/L, then at 4 mmol/L, with a molar ratio of $Mg/NH_4/PO_4$ equal to 1. Crystal size is determined by laser granulometry and morphometry. A population balance-based model coupled with a thermodynamic model predicts particle size distribution vs. experimental time using a reconstruction model. This approach is particularly numerically stable for the identification of nucleation and particle growth kinetics parameters that are used to predict crystal size distribution. The methodology is based on a thermodynamic model previously developed for which pH control and supersaturation constitute key parameters. The obtained results are of major importance for the design of struvite precipitation reactor, and for the development of crystal growth control methodology.

1. Introduction

The cost of environmental protection and pollution prevention is increasing above all because of stringent effluent quality standards. In this context, phosphate impact on water pollution plays a major role since it promotes eutrophication. One proposed solution to this problem is the recovery of phosphate using crystallization. This work addresses the problem of phosphorus recovery from synthetic wastewater by precipitation of struvite. The general objective is to develop a methodology for optimal design of an automated pilot reactor for wastewater treatment.

Two major crystallization processes have been developed for phosphorus recovery from wastewater, respectively the so-called calcium phosphate (CP) precipitation process and the magnesium ammonium phosphate (MAP) or struvite precipitation which is a crystalline substance consisting of magnesium, ammonium and phosphorus in equal molar concentrations ($MgNH_4PO_4{\cdot}6H_2O$). Struvite forms according to the following reaction [1]:

$$Mg^{2+} + NH_4^{+} + PO_4^{3-} + 6H_2O \rightarrow MgNH_4PO_4 \cdot 6H_2O \quad (1)$$

It is important to understand and optimize the precipitation process in order to improve product quality, thus minimizing the associated production costs. A previous study [2–5] based on a thermodynamic model was developed to predict the quantity of

* Corresponding author.
E-mail addresses: Mary.Hanhoun@ensiacet.fr (M. Hanhoun), Ludovic.Montastruc@ensiacet.fr (L. Montastruc), Catherine.AzzaroPantel@ensiacet.fr (C. Azzaro-Pantel), Beatrice.Biscans@ensiacet.fr (B. Biscans), Michele.Freche@ensiacet.fr (M. Frèche), Luc.Pibouleau@ensiacet.fr (L. Pibouleau).

precipitated product under the form of struvite and to determine the evolution of supersaturation and pH with time. Even if conversion rate is an important parameter to control process efficiency, it must be emphasized that crystal size distribution is a key element to control product quality.

Previous studies have shown an influence of pH, mixing energy and solution type on struvite growth rate [1,27,30,31]. However, these studies take into account the mean particle size rather than particle size distribution. The purpose of this study is to evaluate nucleation and growth kinetics laws, using a population balance, and to compare modeling results with experimental particle size distribution.

This paper is organized into four sections.

As mentioned in Section 1 of this paper, the purpose of this study is to develop a methodology to predict particle size distribution. One-dimensional growth modeling in a batch reactor based on nucleation–growth crystal formation is investigated and presented in Section 2. The nucleation model is based on a classical logarithmic formulation proposed by [10,11] depending on supersaturation. The growth model is based on a variable order of supersaturation. In parallel, preliminary experiments were carried out at different initial supersaturation values to determine the induction time and to identify the involved nucleation phenomenon, as well as to evaluate the final particle size distribution in a stirred reactor. Section 3 proposes an innovative strategy based on the classical method of moment [6] to compute nucleation and growth parameters. The major interest of this strategy is to combine a previous developed thermodynamic model [4] and a population balance-oriented one for a more robust determination of these parameters. An optimization procedure was thus carried out, that is based on the minimization of the discrepancy between the experimental supersaturation and the value predicted by the thermodynamic model so as to determine the nucleation and growth parameters. Section 4 is devoted to the identification of nucleation and particle growth kinetics parameters, using the methodology described in Section 3. They are then used to predict the size distribution that is typical of a nucleation–growth model by a reconstruction method [7]. Finally, Section 5 concludes this work and gives some guidelines for struvite precipitation reactor design.

2. General modeling framework

2.1. Coupling a thermodynamic model with a nucleation–growth model

The proposed framework (see Fig. 1) involves a two-step modeling approach. The first step is based on an equilibrium prediction of the studied system $Mg–PO_4–NH_4$ that was developed in a previous work [4]. This model computes the final conversion rate of phosphate (X) as a function of equilibrium pH for different temperatures and supersaturations. From the experimental evolution of pH and the initial concentrations, the model gives the evolution of supersaturation vs. time. This is the starting point for the evaluation of growth and nucleation rates during the second step of the methodology.

The numerical strategy implies a genetic algorithm (NSGA II) [8] both to initialize a classical algorithm of resolution (involving a classical Newton–Raphson method) and to guarantee the robustness of the process. This model requires as inputs the initial concentrations of phosphate, ammonium and magnesium in wastewater, temperature as well as the quantity of sodium hydroxide that is initially added. The phosphate conversion rate X is discretized in the interval bounded by zero and the final conversion rate as upper limit, which then allows the identification of supersaturation with time. Major results are reported in [4]. A second modeling step, which is the core of this investigation involves the development of a nucleation–growth model based on a population balance to predict the kinetic parameters of nucleation and crystal growth of struvite as well as the particle size distribution using the previous developed thermodynamic model.

2.2. Principles of population balance-based modeling

2.2.1. Formulation of population balance equation

This work involves the development of a model of nucleation and growth in a batch reactor. The formalism of the population balance equation to describe the evolution of the crystal size distribution during time in a process of crystallization [9] assumes that neither agglomeration nor breakage occurs and that the expression of growth rate is independent of crystal size. Nucleation rates imply that several phenomena such as homogeneous and heterogeneous nucleation need to be taken into account. The secondary nucleation characterization depends on the degree of mixing in a stirred reactor. The experiments were carried out in a batch reactor with a rotational speed of around 500 rpm at 25 °C. Under these conditions, only primary nucleation occurs with the presence of fines and the crystals grow without agglomeration (no breakage).

$$\frac{\partial n(t,L)}{\partial t} = -G(t,m)\frac{\partial n(t,L)}{\partial L} + r_N(t,m)\times\delta(L-L_0) \tag{2}$$

$$n(t=0, L=0^+) = 1 \quad \text{and} \quad n(t=0,L) = 0$$

In this expression, $m = m(t) > 0$ represents the solute mass in the liquid phase, $n_0(L)$ represents the initial crystal size distribution. $G(t,m)$ is the crystal growth rate that is independent of crystal size; r_N corresponds to the crystal nucleation rate for a minimal size L_0. δ is the Dirac function representing the spontaneous appearance of crystals.

According to the theory of nucleation and growth [10,11], nucleation rate r_N that represents the number of struvite nuclei formed by time unit (s) and volume unit (cm^3) follows the general equation:

$$r_N = A\times\exp\left(\frac{-B}{(\ln\ \Omega)^2}\right)\ (\text{Particle m}^{-3}\ \text{s}^{-1}) \tag{3}$$

The kinetics of crystal growth is expressed by:

$$G = kg\ s^g\ (\text{ms}^{-1}) \tag{4}$$

where A, B, kg, and g are the kinetic parameters to be identified.

Ω is the supersaturation ratio as expressed by:

$$\Omega = \left(\frac{a_{Mg^{+2}}\cdot a_{NH_4^+}\cdot a_{PO_4^{3-}}}{K_{sp}}\right)^{\frac{1}{3}} \tag{5}$$

a_i represents the ionic activity of species i related to struvite in the solution. K_{sp} is struvite solubility product, which was determined equal to $10^{-13.17}\ (\text{mol/L})^3$ at 25 °C in [4].

In general, the population balance involves differential equations to model the population density distribution. Many examples such as [12,9,13–16] can be found. Analytical solutions of the population balance equation can be obtained only for simple cases. Yet, a numerical solution is required in the majority of cases.

In that context, the method of moments is one of the simplest available techniques for solving the population balance equation. It transforms the population balance equation into a set of ordinary differential equations in terms of moments of size distribution. It makes it possible to use the experimental crystal size distributions directly with a good compromise between precision and speed of resolution. This method was chosen here to develop a model of nucleation–growth of struvite in a perfectly stirred reactor starting from a population balance equation under the assumption that neither agglomeration nor breakage occurs. It must be emphasized

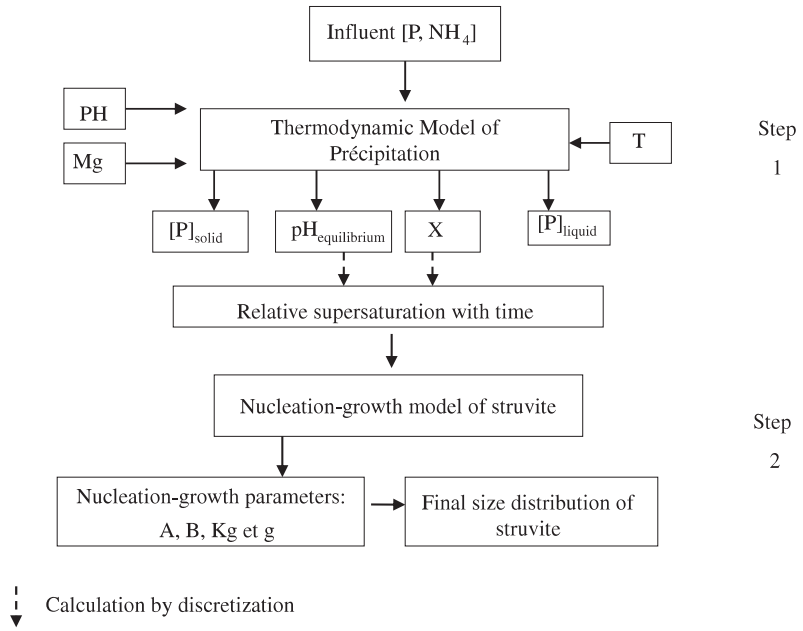

Fig. 1. Principles of reactor modeling.

that no agglomeration was mentioned in the work of [17] which is in agreement with the assumption that is considered here: struvite has negative potential zeta in the range of pH (8.5–10.5). It must be highlighted that some crystal samples were collected along batch evolution and do not exhibit the presence of dust (fines) or broken crystals.

Since the condition of supersaturation is verified here, nucleation (or germination) can occur. The nuclei (or germs) are the smallest crystals that are thermodynamically stable. To understand the nucleation process, it is thus necessary to investigate the kinetic mechanisms leading to the formation of nuclei. The terminology suggested by Mullin [10] is adopted in this work. The involved mechanisms depend on the explored operating conditions during nucleation and on the physicochemical properties of the medium. Primary nucleation concerns the formation of the new solid phase that occurs in systems that do not contain previously crystalline materials. Two types of primary nucleation are generally distinguished: (i) homogeneous primary nucleation for which the new solid phase appears starting from a supersaturated solution that is free from any impurity; and (ii) heterogeneous primary nucleation for which the formation of the new solid phase is catalyzed by the presence of some impurities in the solution.

In most cases [10], as in this work, nucleation cannot be homogeneous (primary) and nucleation is initiated either by suspended particles or by the walls of the reactor.

In some specified cases, the phenomena of nucleation are preceded by the so-called induction time.

2.2.2. Population balance resolution by the method of the moments

Eq. (2) cannot be solved analytically. The population balance can be transformed by the method of moments by writing the *k*th-order moment noted μ_k, as follows:

$$\mu_k(t) = \int_0^\infty L^k n(t, L))dL \tag{6}$$

The moments are computational tools leading to the characteristics of particle sizes

$$\mu_0 = \int_0^\infty n(L)dL = NT \tag{7}$$

In this expression, N_T represents the total number of particles.

To determine the particle size distribution number, the evolution of the 0th-order moment is thus required.

$$\mu_1 = \int_0^\infty L \times n(L)dL \Rightarrow L_T = \phi_L \frac{\mu_1}{\mu_0} \tag{8}$$

L_T indicates the mean particle size and ϕ_L is the size shape factor (ϕ_L = 1 in the case of spheres).

$$\mu_2 = \int_0^\infty L^2 \times n(L)dL \Rightarrow A_T = \phi_A \frac{\mu_2}{\mu_0} \tag{9}$$

A_T is the average surface of the particles and ϕ_A is the surface shape factor of form (ϕ_A = √1 in the case of sphere).

$$\mu_3 = \int_0^\infty L^3 \times n(L)dL \Rightarrow V_T = \phi_V \frac{\mu_3}{\mu_0} \tag{10}$$

V_T indicates the volume average particle volume and Φ_V is the volume shape factor (ϕ_V = √1/6 in the case of sphere).

According to [18], the mass balance in the liquid phase can be expressed as follows:

$$\frac{dm(t)}{dt} = -3\rho_C \phi_V G(t, m) \times \mu_2(t) \tag{11}$$

where ρ_C is the crystal density, ϕ_V is the volume shape factor. SEM imagery makes it possible to observe the formed crystal shape. The shape factor is fixed at 0.01 to take into account the needle form, as proposed in [6] and confirmed by our observations (see Fig. 8). Kinetics values are of course related to the assumptions made for the shape factor value.

By using the definition of the moments (Eq. (6)), the population balance Eq. (2) and the mass balance (11), a system of ordinary differential equations [6,19–24] is obtained:

$$\frac{D\mu_0(t)}{dt} = r_N(t, m) \tag{12}$$

$$\frac{d\mu_k(t)}{dt} = i \times G(t, m) \times \mu_{k-1}(t) \tag{13}$$

$$m(t) + \rho_C \phi_V \mu_3(t) = m(t_0) + \rho_C \phi_V \mu_3(t_0) \tag{14}$$

The initial values of the moment and the solute mass are positive:

$$\mu_i(t_0) \geqslant 0,\ m(t_0) \geqslant 0, \quad i = 0, 1, 2, 3$$

The mass of the formed crystal m is not usually used in the field of crystallization. It is thus necessary to express the distribution size number as a function of the number of crystal moles that are formed under conditions of supersaturation. Then, the laws of growth and nucleation rate are written according to the medium supersaturation. Absolute supersaturation "s" ($s = (a_{NH_4} \times a_{PO_4} \times a_{Mg})^{1/3} - K_{sp}^{1/3}$) makes it possible to obtain the number of crystal moles per volume unit that can be formed at equilibrium state. The use of supersaturation in the material balance implies that the equilibrium is achieved at date t. By dividing the mass balance Eq. (14) by the molar mass M_C of the formed crystal, the following expression is then obtained:

$$s(t) + \frac{\rho_C \phi_V}{M_c}\mu_3(t) = s(t_0) + \frac{\rho_C \phi_V}{M_c}\mu_3(t_0) \tag{15}$$

The resolution of the resulting ordinary differential equation system (Eqs. (12) and (13)) allows the computation of the evolution of the 3rd order moment (μ_3) vs. time. Eq. (15) leads to the evolution of the absolute supersaturation with time.

3. Methodology for determination of nucleation and crystal growth kinetic parameters

The objective of this section is to present how the thermodynamic model that was developed in a previous work can be used to determine the evolution of supersaturation with time from the computation of pH and species concentration assuming that a quasi-equilibrium state is reached. Indeed, for initial pH and a given wastewater quality, it is possible to compute the phosphorus conversion rate at steady state, and thus, the associated supersaturation and pH. Briefly, the thermodynamic model developed in [4] allows the computation of the evolution of pH vs. time using supersaturation.

The kinetic constants of nucleation and growth of struvite can be determined by minimizing the squared difference between the experimental and computed supersaturation values. This method does not require the use of a granulometric analysis, but is sensitive to the accuracy of the thermodynamic model. To our knowledge, this type of approach has not yet been explored in the dedicated literature. The kth order moment depends on the crystal density number "n". It is therefore possible to compute this density number by mathematical methods for moment inversion of order K "μ_k" (Eq. (6)). The evolution of the absolute supersaturation vs. time is calculated by solving the involved differential equations using the following equation:

$$s(t) + \frac{\rho_C \phi_V}{M_c}\mu_3(t) = s(t_0) + \frac{\rho_C \phi_V}{M_c}\mu_3(t_0) \tag{16}$$

The methodology is explained as follows (see Fig. 2):

- For each experiment (concentration of Mg, NH_4, PO_4 and different pH values), the relative supersaturation ($Sr = s/Ce$: s is the absolute supersaturation, $s = (a_{NH_4} \times a_{PO_4} \times a_{Mg})^{1/3} - K_{sp}^{1/3}$, Ce is the solubility of struvite, $Ce = K_{sp}^{1/3}$) in the domain of pH variation is calculated. This domain is discretized with a constant step equal to 0.001.
- This step is followed by an interpolation using a polynomial model to obtain a continuous function $Sr = f(\text{pH})$.
- Then, the value of supersaturation is computed for the experimental pH value $Sr_{exp} = f(\text{pH}_{exp})$ using the function $Sr = f(\text{pH})$. The experimental supersaturation vs. time $Sr_{exp} = f(\text{t})$ is finally obtained.

The determination of the parameters A, B, kg and g using experimental data is carried out by minimizing the quadratic function as follows:

$$\begin{aligned} &\text{Min}[F(A, B, kg, g)] \\ &\text{With} \\ &F(A, B, kg, g) = \sum_{N_{exp=1}}^{n} \sum_{t=1}^{tend} \left[Sr^i_{\text{Model}}(t) Sr^i_{\text{Exp}}(t) \right]^2 \end{aligned} \tag{17}$$

N_{exp} is the number of experiments, t the time corresponding to an experimental point, t_{end} the time at the end of an experiment, and Sr is the relative supersaturation obtained by the resolution of the set of differential equations: experimental relative supersaturation is calculated by the thermodynamic model for initial concentrations of [Mg], [PO_4], [NH_4] and pH at time t.

The resolution of the abovementioned optimization problem gives the kinetic parameters of nucleation and growth rate values for struvite. Since the problem belongs to the class of nonlinear optimization, it is necessary at first time to explore a large space because many local minima may exist. Then, a growth rate expression that is valid for all the experiments is identified. Finally, the experimental crystal size distribution is compared with the computed ones by use of the method of reconstruction of the crystal size distribution, as explained in the Electronic annex (reconstruction of crystal size distribution section).

4. Experimental determination of nucleation and crystal growth kinetic parameters

4.1. Induction time

The induction time corresponds to the time between the establishment of supersaturation and the occurrence of first nuclei. It depends directly on the degree of supersaturation, temperature and the presence of impurities in the solution. Its experimental measurement is not straightforward and depends strongly on the sensibility of the sensor, that is to say a pH-meter [1], turbidimeter [25], absorption measurement [26]. According to [27], the induction time is inversely proportional to nucleation rate (either homogeneous or heterogeneous).

$$t_{ind} \propto \frac{1}{r_N} \tag{31}$$

When combining Eqs. (3) and (31) and applying the log transformation, we obtained the following equation:

$$\ln(t_{\text{induction}}) = \frac{B}{(\ln(\Omega))^2} - \ln(A') \tag{32}$$

The parameter B is described in Eq. (3) and A' is a function of parameter A (Eq. (3)).

The induction time can be observed through experiments, between the beginning of an experiment and the beginning of variation of solution pH, which corresponds to the beginning of crystal growth and the end of the induction period. The value of t_{ind} allows a direct determination of the values of the kinetic parameters both for homogeneous or heterogeneous nucleation.

4.2. Experimental determination of the nucleation rate constant

Experiments were carried out at different initial supersaturation values in a stirred reactor (3L) at a rotational speed of around 500 rpm with 25 °C. Stock solutions of magnesium and ammonium phosphate were prepared from corresponding crystalline solids, i.e., $MgCl_2{\cdot}6H_2O$ and $NH_4H_2PO_4$. Deionised water was used to prepare the synthetic wastewater solution. The supersaturated

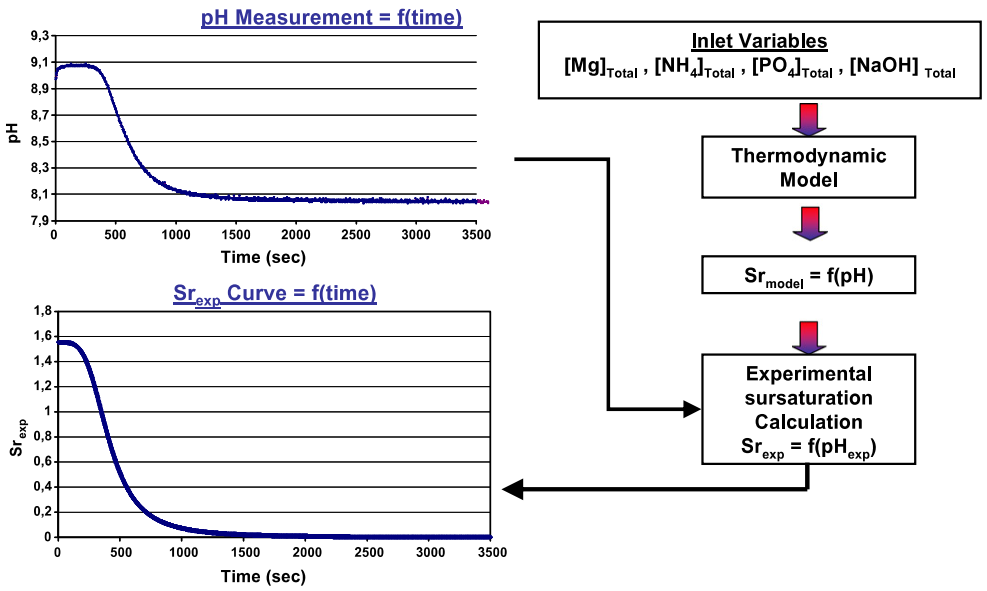

Fig. 2. Method of experimental determination of supersaturation.

solutions (corresponding to a final phosphorus concentration of respectively 3 and 4 mmol/L) with a $Mg/NH_4/PO_4$ molar ratio equal to 1 were prepared by rapid mixing of $NH_4H_2PO_4$ and pH was then adjusted by the addition of the appropriate amount of a standard solution of sodium hydroxide, followed by the addition of the appropriate volume of stock magnesium chloride solution. The reaction is studied in supersaturation range $1.83 < \Omega < 3.44$. The initial concentrations of Mg, PO_4 and NH_4 are first fixed at 3 mmol/L, then at 4 mmol/L, with variable initial pH comprised between 8.5 and 9.5 and with an $Mg/NH_4/PO_4$ molar ratio equal to 1. Each experimental point is repeated three times for guaranteeing repeatability, and these three values are inserted in the computation for identification. The experimental points are available in the Electronic annex.

The induction times were defined as being the duration starting from the initial mixture of the solutions until the first change of pH corresponding to the beginning of precipitation, for this reason, the pH is selected as the indicator of precipitation. The mixing time (6.6 s) is not negligible as compared to the induction time in the case of homogeneous nucleation. The lowest value of the induction time is about 15 s, which corresponds to both mixing and induction time. This is why the parameter B obtained from the experiments i.e., 9.93 (respectively 0.9) for homogeneous (respectively heterogeneous) nucleation is only used to have an order of magnitude to calculate the parameters of nucleation and growth rate of struvite.

In Fig. 3, two zones can be observed, corresponding to both mechanisms of primary nucleation that are homogeneous and heterogeneous. The transition between homogeneous and heterogeneous occurs at a value of $\frac{1}{(\ln\ \Omega)^2}$ equal to 0.96, which leads to a supersaturation ratio Ω lower than 2.68.

The value of the parameter B determined during this study (Fig. 3) is used to check the order of magnitude of this parameter. The next stage concerns the determination of struvite crystal growth rate.

4.3. Variation domain of the parameters for nucleation and crystal growth

The optimization of nucleation and growth rate parameters requires the determination of the variation domain of these parameters. Let us recall that the objective is to find the parameters allowing at the same time to have an evolution according to the time of relative supersaturation that is in agreement with the experimental profile.

A value of A equal to 10^{23} $m^3\ s^{-1}$ is proposed in the literature [28] without yet specifying the conditions under which this value is given. During some preliminary tests, by taking this value as a reference, the results were very far from the experimental ones. A sensitivity analysis for these parameters was thus performed.

The following strategy was implemented:

- The value of the parameter g is fixed at 2 (when growth is controlled by integration, the value of g is comprised between 1 and 2).
- The value of parameter A is changed "manually" between 10^6 and 10^{23}.

Then, the parameters B and k_g are given so that the relative supersaturation vs. time as predicted by the model takes the nearest possible value of the experimental ones (cf. Fig. 2). Figs. 4 and 5 present the variations of parameters A, B and k_g for homogenous and heterogeneous nucleation. From this basis, the parameter range can be determined:

- Parameter A: the maximum crystal size obtained in the experimental runs (SEM observations and morphometry) is about 70 μm for homogeneous nucleation and reaches 75 μm for heterogeneous nucleation. It can thus be assumed that parameter A can vary between 10^8 and 10^{13} for homogeneous nucleation, (respectively between 10^6 and 10^9 for heterogeneous nucleation).
- Parameter B: is comprised between 7 and 8 for homogeneous nucleation, (respectively between 0 and 1 for heterogeneous nucleation). These values are confirmed by the induction time values obtained in experimental runs.
- Parameter k_g varies between 10^{-8} and 10^{-3} $m\ s^{-1}$ for homogeneous nucleation (respectively between 10^{-6} and 10^{-3} $m\ s^{-1}$ for heterogeneous nucleation).

Table 1 shows the variation domains used to optimize these parameters.

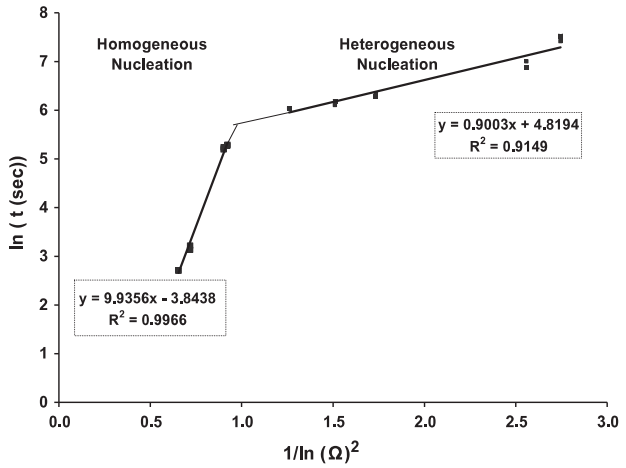

Fig. 3. Evolution of induction time logarithm vs. supersaturation.

4.4. Calculation of the kinetic parameters for homogeneous and heterogeneous nucleation and growth

The determination of the parameters for the general growth rate requires to take into account all the experimental series in the optimization phase and also to distinguish the series for which homogeneous nucleation (respectively heterogeneous) occurs and consequently to compute the parameter A relative to each type of phenomenon. For all the series, whatever the nucleation, the growth rate is identical, which implies that the parameters of growth, that are k_g and g take relevant values. The optimization results of the parameters A, B, k_g and g (homogeneous and heterogeneous nucleation) are presented in Table 2 for the whole set of experimental runs.

The range of g is found between 1.46 and 1.68 [29] but does not consider the type of nucleation. The value of g equal to 1.34 in our experiments exhibits the same order of magnitude but is slightly lower. Experimental and calculated supersaturation values are compared in Figs. 6a–6c and 7a–7d for various initial supersaturation values corresponding both to homogeneous and heterogeneous nucleation. The feasibility of the method proposed here is demonstrated since it is possible to obtain parameters in agreement with the actual evolution of supersaturation in the reactor, thus leading to parameters of nucleation and growth that are consistent with thermodynamics. It can be observed that a very close agreement between the experimental supersaturation and the predicted one is obtained. From a numerical point of view, the methodology is more stable when calculating the parameters of the nucleation rate and growth for all series simultaneously.

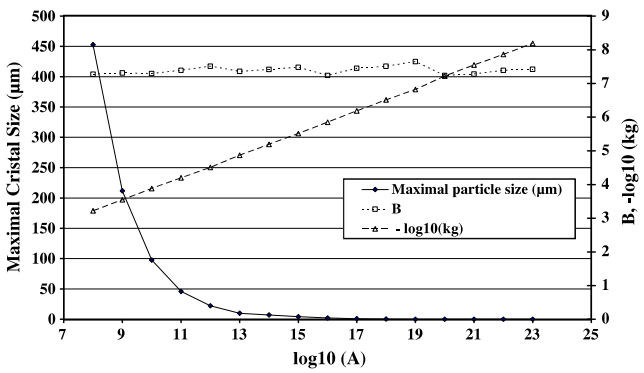

Fig. 4. B and k_g parameters sensitivity with A value for homogeneous nucleation.

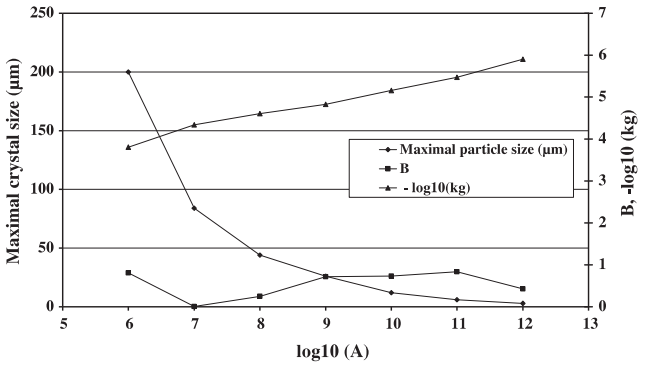

Fig. 5. B and k_g parameter sensibility with A value for heterogeneous nucleation.

4.5. Reconstruction of size distribution

The results obtained by the numerical method of reconstruction of the size distribution are now compared with those obtained with experimental analysis, ie., laser granulometry and morphometry. It must be emphasized that laser granulometry is not well-suited for considering non-spherical crystals. It is yet necessary to take into account the shape of crystals and the mode of growth. For this purpose, some images of the obtained crystals are achieved by means of Scanning Electron Microscope SEM. The observations (Fig. 8) confirm that crystals of big size are obtained (up to 180 µm) and also show the formation in large quantities of crystal aggregates of small size. The aggregation phenomenon is probably the origin of the difference in the forms of the size distribution. During aggregation, crystal growth is not due to the surface growth of the crystal but to an addition of crystals of small size.

Morphometry, based on image analysis principle, as well as SEM characterizes particles by providing high-quality images that are very precise from a statistical point of view on the size and particle shape. Morphometry G3 is an ideal technology to detect the presence of an extremely low number of particles or foreign bodies. The particle size, which can be measured ranges between 0.5 µm and 3000 µm. For each experimental series, it is possible to reconstitute the final size distribution numerically, by using the abovementioned procedure for the experiments with either homogeneous or heterogeneous nucleation (Fig. 9). The results are then compared with those obtained by laser granulometry for homogeneous and heterogeneous nucleation (Fig. 10). The modeled size distribution is also compared with the morphometric analysis (Fig. 11). It can be pointed out that the particle sizes provided by laser granulometry are larger than those predicted by the numerical approach. Moreover, the size distribution exhibits different shapes for experiments and simulation runs. The maximum volumetric percentage corresponds to the maximum size predicted by the model of reconstruction of size distribution. The volumetric percentage predicted by the model of reconstruction and that obtained by laser granulometry are identical. The size distribution form obtained by morphometric analysis (Fig. 11) is closer to that

Table 1
Variation domain of the parameters for nucleation and crystal growth.

	Homogeneous		Heterogeneous	
	Minimal	Maximal	Minimal	Maximal
A (m^{-3} s^{-1})	10^8	10^{13}	10^6	10^{10}
B	6	10	0	2
	Minimal		Maximal	
k_g (m/s)	10^{-7}		10^{-3}	
g	1		2	

Table 2
Kinetic parameters of homogeneous and heterogeneous nucleation and growth.

	Homogeneous Nucleation and growth	Heterogeneous
A ($m^{-3}\ s^{-1}$)	$10^{9.6}$	$10^{7.47}$
B	449	0.6
k_g (m/s)	$10^{-5.33}$	$10^{-5.33}$
g	1.34	1.34

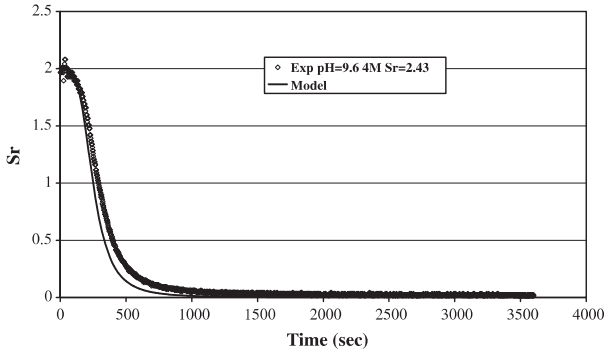

Fig. 6a. Comparison of the predicted and experimental values with time for homogeneous primary nucleation (pH initial = 9.6, $[NH_4] = [PO_4] = [Mg]$ = 4 mmol/L, *Sr* initial = 2.43).

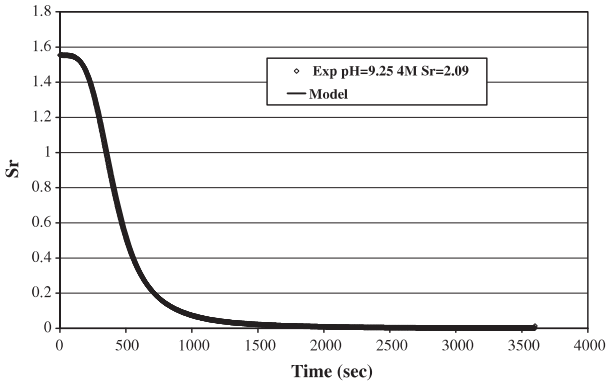

Fig. 6b. Comparison of the predicted and experimental values with time for homogeneous primary nucleation (pH initial = 9.25, $[NH_4] = [PO_4] = [Mg]$ = 4 mmol/L, *Sr* initial = 2.09).

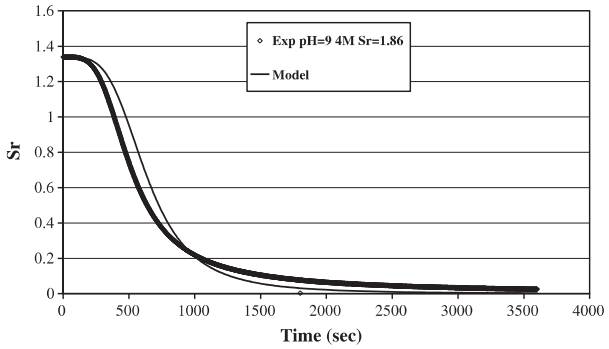

Fig. 6c. Comparison of the predicted and experimental values with time for homogeneous primary nucleation.

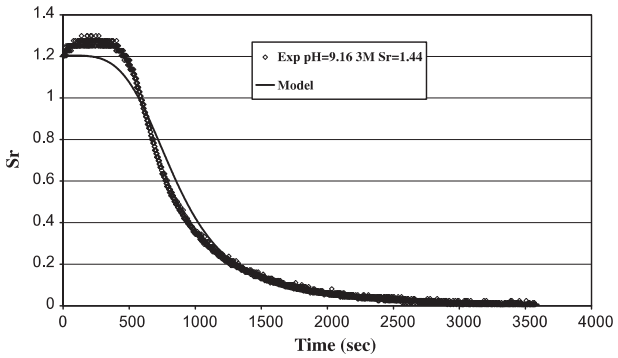

Fig. 7a. Comparison of the predicted and experimental supersaturation for heterogeneous primary nucleation (pH initial = 9.16, $[NH_4] = [PO_4] = [Mg]$ = 3 mM/L, *Sr* initial = 1.44).

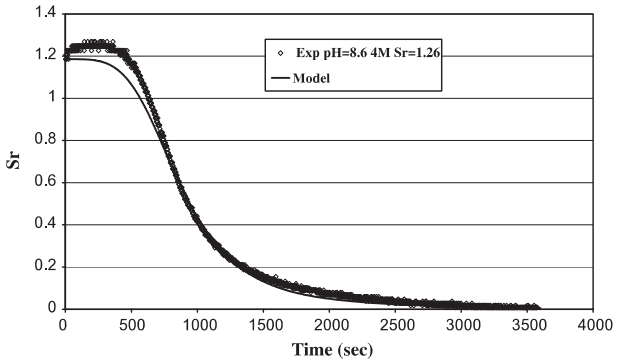

Fig. 7b. Comparison of the predicted and experimental supersaturation for heterogeneous primary nucleation (pH initial = 8.6, $[NH_4] = [PO_4] = [Mg]$ = 4 mmol/L, *Sr* initial = 1.26).

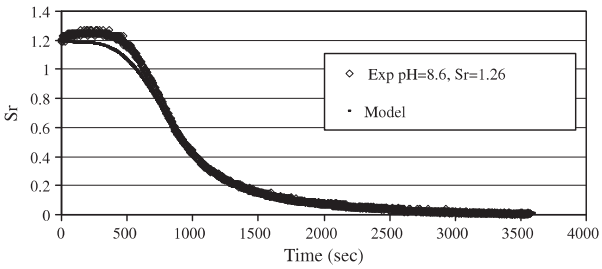

Fig. 7c. Comparison of the predicted and experimental supersaturation for heterogeneous primary nucleation (pH initial = 8.5, $[NH_4] = [PO_4] = [Mg]$ = 3 mmol/L, *Sr* initial = 0.87).

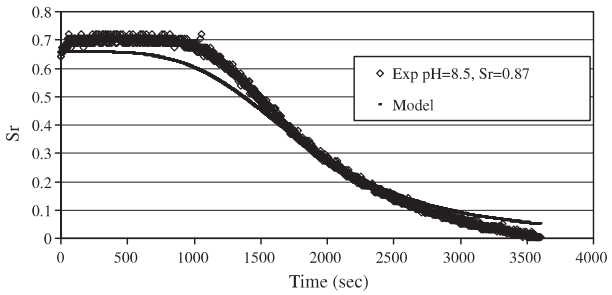

Fig. 7d. Comparison of the predicted and experimental supersaturation for heterogeneous primary nucleation.

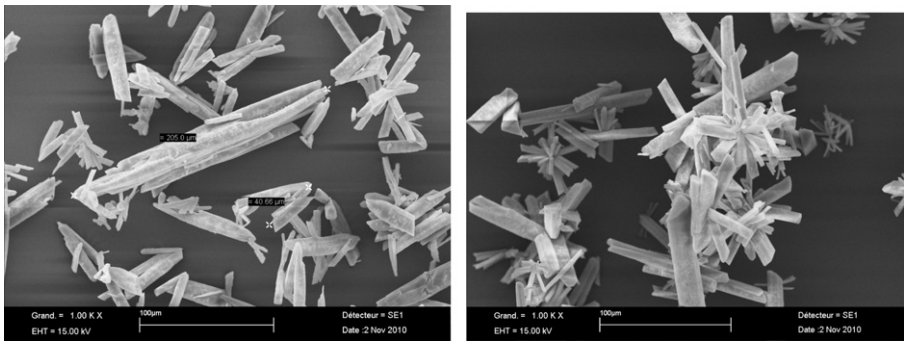

Fig. 8. Struvite crystal at the end of crystallization.

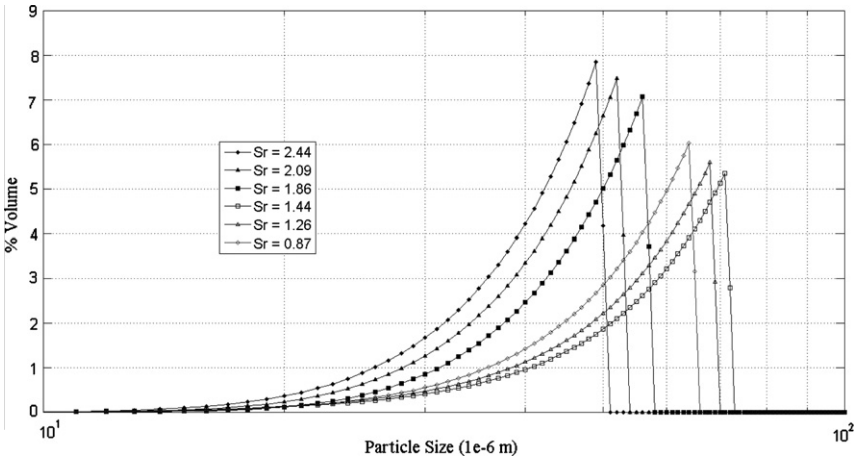

Fig. 9. Reconstruction of particle size distribution (*Sr* initial between 0.87 and 2.44).

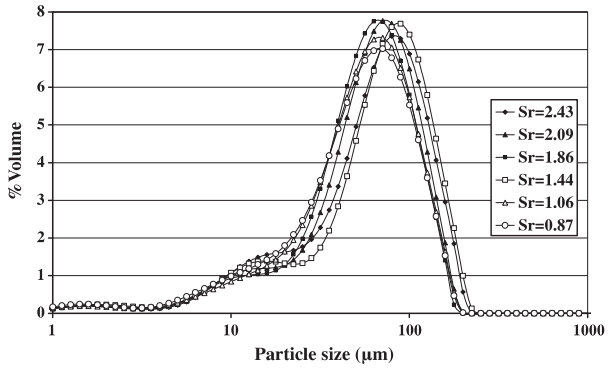

Fig. 10. Particle size distribution for various initial supersaturation values by laser granulometry (*Sr* initial between 0.87 and 2.44).

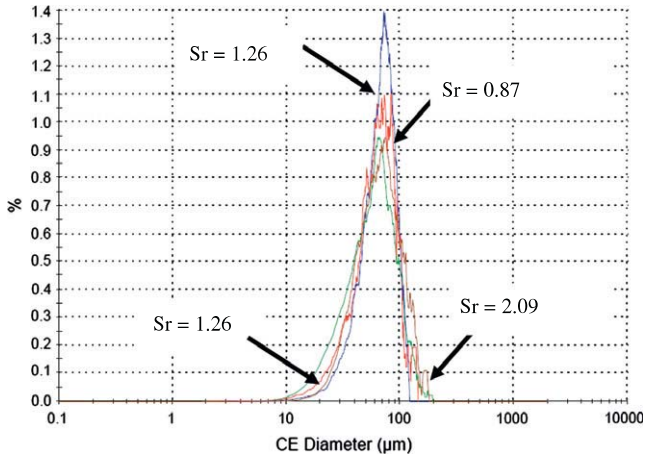

Fig. 11. Particle size distribution for various initial supersaturation by morphometry.

obtained by the reconstruction model. The volumetric percentage from morphometric analysis is lower than that given by laser granulometry or predicted by the reconstruction model.

An important parameter concerns the size of the crystals that are mainly produced during crystallization. Table 3 presents the comparison between the crystal size produced during the experiments (the size corresponds to the maximum value of the volumetric percentage) and the values obtained by the numerical method of reconstruction of size distribution. It can be highlighted that the method of reconstruction in the case of a heterogeneous nucleation induces a better precision level. The difference between model results and experiments is more important in the case of homogeneous nucleation.

More generally, the results obtained by morphometry are closer to the results of the reconstruction model. In case of heterogeneous nucleation, the accuracy lies between 1% and 5%, and in case of homogeneous nucleation, the accuracy is between 15% and 20%.

The variation is much more important when comparing with the results given by laser granulometry: for heterogeneous

Table 3
Comparison between the crystal size corresponding to the maximum value of volumetric percentage (mode of the distribution obtained for the experiments with the reconstruction model).

	Morphometry (μm)	Laser granulometry (μm)	Model size (μm)	Deviation between model and morphometry measurement (%)	Deviation between model and laser granulometry measurement (%)
Homogeneous nucleation					
Sr = 2.43	58	89	49	15.71	−44.94
Sr = 2.09	66	80	53	19.70	−33.75
Sr = 1.86	68	71	55	19.12	−22.54
Heterogeneous nucleation					
Sr = 1.44	74	90	70	5.41	−22.22
Sr = 1.06	68	71	67	1.47	−5.63
Sr = 0.87	62	70	64	−3.23	−8.57

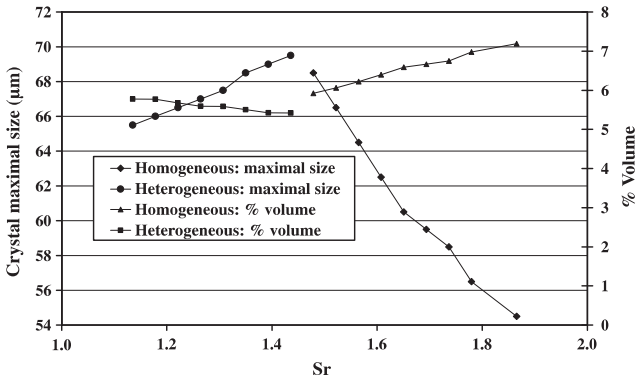

Fig. 12. Maximum crystal size calculated by the reconstruction method of size distribution according to the relative supersaturation of the medium.

nucleation, the accuracy is between 5% and 22%, and in case of homogeneous nucleation, the accuracy is between 20% and 45%.

These results demonstrate the possibility to predict the distribution and the maximum size of crystals with a numerical reconstruction of particle size distribution, starting from nucleation and growth kinetics determined in a stirred reactor.

4.6. Determination of optimal supersaturation for struvite growth

The design of an efficient process for water treatment requires the production of crystals of important size to avoid a subsequent filtration stage, with relatively low concentrations of phosphates, ammonium and magnesium and, consequently, a minimal supersaturation of the solution. The reconstruction model of the size distribution predicts the maximum size that struvite can reach according to the initial conditions. The type of nucleation influences the final crystal size (see Fig. 12). For homogeneous nucleation, an increase in relative supersaturation results in a decrease in the maximum crystal size obtained while the volumetric percentage yet increases. Conversely, for heterogeneous nucleation, an increase in relative supersaturation involves an increase in the maximum crystal size while the volumetric percentage yet decreases. It can be deduced that there exists a compromise between the maximum crystal size and a minimal supersaturation value, corresponding to a value of intermediate supersaturation between homogeneous and heterogeneous nucleation. The reconstruction model of the size distribution makes it possible to carry out a study of the maximum crystal size sensibility obtained in function of relative supersaturation.

Fig. 12 presents the maximum crystal size predicted by the reconstruction model of size distribution vs. relative supersaturation. It can be observed that a relative supersaturation of 1.455 leads to a maximum crystal size of 69.5 μm, which also corresponds to the maximum volumetric percentage of the produced crystals.

5. Conclusion

The crystal size distribution prediction is a cornerstone to control the quality of a precipitated product. For this purpose, a population balance to predict the particle size distribution was developed and a simplified nucleation–growth crystal formation was studied, based on a one-dimensional model of batch crystallization.

A new strategy has been implemented for a robust determination of the parameters of nucleation and growth, coupling a thermodynamic model which was developed in previous investigations with a population balance equation. An optimization procedure based on the minimization of squared difference between supersaturation predicted by the model of growth and the value obtained from experiments was implemented in order to identify the parameters of nucleation and growth.

The results are in agreement with the evolution of supersaturation along time in the reactor. From a numerical point of view, this approach has proved to be more stable numerically when considering all the experimental series for identifying the parameters of nucleation rate and growth. These parameters were then used to predict the size distribution using a method of reconstruction. The shape of the crystal size distribution obtained by calculation is typical of a nucleation–growth model where the growth phenomena of aggregation and breakage of the crystals are neglected. The reconstruction method also exhibits a good agreement with the curves of size distribution obtained by laser granulometry and morphometry. The results obtained by morphometry are more realistic and closer to the results of the reconstruction model: for heterogeneous nucleation, the accuracy is between 1% and 5%, and in the case of homogeneous nucleation, the accuracy is between 15% and 20%.

These results are of major importance for the design of struvite precipitation reactor and for the development of crystal growth control methodology.

Appendix A. Supplementary material

Supplementary data associated with this article can be found, in the online version, at http://dx.doi.org/10.1016/j.cej.2012.10.038.

References

[1] N.C. Bouropoulos, P.G. Koutsoukos, Spontaneous precipitation of struvite from aqueous solutions, J. Cryst. Growth 213 (2000) 381–388.
[2] M. Hanhoun, C. Azzaro-Pantel, B. Biscans, M. Freche, L. Montastruc, L. Pibouleau, S. Domenech, Removal of Phosphate from synthetic wastewater by struvite precipitation in a stirred reactor, COVAPHOS III 6 2009 100–106.
[3] M. Hanhoun, C. Azzaro-Pantel, B. Biscans, M. Freche, L. Montastruc, L. Pibouleau, S. Domenech, A thermochemical approach for Struvite

precipitation modelling from wastewater, in: International Conference on Nutrient Recovery from Wastewater Streams, Vancouver, Canada, 2009.
[4] M. Hanhoun, L. Montastruc, C. Azzaro-Pantel, B. Biscans, M. Freche, L. Pibouleau, Temperature impact assessment on struvite solubility product: a thermodynamic modeling approach, Chem. Eng. J. 167 (2011) 50–58.
[5] L. Montastruc, C. Azzaro-Pantel, L. Pibouleau, S. Domenech, Use of genetic algorithms and gradient based optimization techniques for calcium phosphate precipitation, Chem. Eng. Process. 43 (2004) 1289–1298.
[6] E. Barbier, M. Coste, A. Genin, D. Jung, C. Lemoine, S. Logette, H. Muhr, Simultaneous determination of nucleation and crystal growth kinetics of gypsum, Chem. Eng. Sci. 64 (2009) 363–369.
[7] S. Qamar, Modeling and simulation of population balances for particulate processes, HDR, Faculty of Mathematics Otto-von-Guericke University, Magdeburg, 2008.
[8] K. Deb, A. Pratap, S. Agarwal, T. Meyarivan, A fast and elitist multiobjective genetic algorithm: NSGA-II, IEEE Trans. Evol. Comput. 2 (2002) 182–197.
[9] A. Randolph, M.A. Larson, Theory of Particulate Processes, second ed., Academic Press, Inc., San Diego, CA, 1988.
[10] J.W. Mullin, Crystallisation, fourth ed., Butterworth Heinemann, Oxford, 2002.
[11] A.E. Nielsen, Kinetics of Precipitation, Pergamon, Oxford, UK, 1964.
[12] H.M. Hulburt, S. Katz, Some problems in particle technology, Chem. Eng. Sci. 19 (1964) 555–574.
[13] S. Kumar, D. Ramkrishna, On the solution of the population balance equations by discretization – I. A fixed pivot technique, Chem. Eng. Sci. 51 (1996) 1311–1332.
[14] S. Kumar, D. Ramkrishna, On the solution of population balance equations by discretization – III. Nucleation, growth and aggregation of particles, Chem. Eng. Sci. 52 (1997) 4659–4679.
[15] G. Madras, B.J. McCoy, Reversible crystal growth–dissolution and aggregation breakage: numerical and moment solutions for population balance equations, Powder Technol. 143–144 (2004) 297–307.
[16] R. Gunawan, D.L. Ma, M. Fujiwara, R.D. Braatz, Identification of kinetic parameters in a multidimensional crystallization process, Int. J. Mod. Phys. B 16 (2002) 367.
[17] K.S. Le Corre, E. Valsami-Jones, P. Hobbs, S.A. Parsons, Impact of reactor operation on success of struvite precipitation from synthetic liquors, Environ. Technol. (2006).
[18] S.M. Miller, J.B. Rawlings, Model identification and quality control strategies for batch cooling crystallizers, AIChE J. 40 (1994) 1312–1327.
[19] S. Qamar, G. Warnecke, Simulation of multicomponent flows using high order central schemes, Appl. Num. Math. 52 (2004) 183–201.
[20] S. Qamar, G. Warnecke, A high order kinetic flux-spitting method for the special relativistic magnetohydrodynamics, J. Comput. Phys. 205 (2005) 182–204.
[21] S. Qamar, G. Warnecke, Application of space-time CE/SE method to shallow water magnetohydrodynamics equations, J. Comput. Appl. Math. 196 (2006) 132–149.
[22] S. Qamar, G. Warnecke, A space-time conservative method for hyperbolic systems with stiff and non stiff source terms, Commun. In Comput. Phys. (CiCP) 1 (2006) 451–480.
[23] S. Qamar, M.P. Elsner, I. Angelov, G. Warnecke, A. Seidel-Morgenstern, A comparative study of high resolution schemes for solving population balances in crystallization, Comput. Chem. Eng. 30 (2006) 1119–1131.
[24] U. Vollmer, Control of crystallization based on population balances, Ph.D. Thesis, Faculty of Electrical Engineering and Information Technology, Otto-von-Guericke University, 2005.
[25] O. Söhnel, J.W. Mullin, A method for the determination of precipitation induction periods, J. Cryst. Growth 44 (1978) 377–382.
[26] I. Kabdasli, S.A. Parsons, O. Tunay, Effect of major ions on induction time of struvite precipitation, Croat. Chem. Acta 79 (2006) 243–251.
[27] K.N. Ohlinger, T.M. Young, E.D. Schroeder, Kinetics effects on preferential struvite accumulation in wastewater, J. Environ. Eng. 125 (1999) 730–737.
[28] F. Abbona, H.E. Lundager, L. Madsen, R. Boistelle, Crystallization of two magnesium phosphates, struvite and newberyite: effect of ph and concentration, J. Cryst. Growth 57 (1982) 6–14.
[30] Md.I. Ali, P.A. Schneider, An approach of estimating struvite growth kinetic incorporating thermodynamic and solution chemistry, kinetic and process description, Chem. Eng. Sci. 63 (2008) 3514–3525.
[30] J. Koralewska, K. Piotrowski, B. Wierzbowska, A. Matynia, Kinetics of reaction-crystallization of struvite in the continuous draft tube magma type crystallizers, Prod. Eng. Chem. Technol. 17 (2) (2009) 330–339.
[32] A.N. Kofina, P.G. Koutsoukos, Spontaneous precipitation of struvite from synthetic wastewater solutions, Cryst. Growth Des. 5 (2005) 489–496.